



Published in final edited form as:

Cell. 2014 April 24; 157(3): 664–675. doi:10.1016/j.cell.2014.02.026.

Merkel cells transduce and encode tactile stimuli to drive A β -afferent impulses

Ryo Ikeda, Myeounghoon Cha, Jennifer Ling, Zhanfeng Jia, Dennis Coyle, and Jianguo G. Gu*

Department of Anesthesiology, The University of Cincinnati College of Medicine, 231 Albert Sabin Way, Cincinnati, OH 45267-0531, USA

SUMMARY

Sensory systems for detecting tactile stimuli have evolved from touch-sensing nerves in invertebrates to complicated tactile end-organs in mammals. Merkel discs are tactile end-organs consisting of Merkel cells and A β -afferent nerve endings, and are localized in fingertips, whisker hair follicles and other touch-sensitive spots. Merkel discs transduce touch into slowly adapting impulses to enable tactile discrimination, but their transduction and encoding mechanisms remain unknown. Using rat whisker hair follicles, we show that Merkel cells rather than A β -afferent nerve endings are primary sites of tactile transduction, and identify the Piezo2 ion channel as the Merkel cell mechanical transducer. Piezo2 transduces tactile stimuli into Ca²⁺-action potentials in Merkel cells, which drive A β -afferent nerve endings to fire slowly adapting impulses. We further demonstrate that Piezo2 and Ca²⁺-action potentials in Merkel cells are required for behavioral tactile responses. Our findings provide insights into how tactile end-organs function and have clinical implications for tactile dysfunctions.

Keywords

Merkel cell; tactile end-organ; mechanotransduction; Piezo2 ion channel; whisker hair follicle

INTRODUCTION

The sense of touch is indispensable for environmental exploration, social interaction, tactile discrimination and other tasks in life. Much of what we know about the transduction and encoding of touch stimuli is from the study of invertebrates' simple touch-sensing nerves (Chalfie and Au, 1989; Kernan et al., 1994; Yan et al., 2013). In contrast to invertebrates, mammals have developed complicated tactile end-organs in the skin including Merkel discs,

© 2014 Elsevier Inc. All rights reserved.

*Correspondence to: gujo@uc.edu.

SUPPLEMENTAL INFORMATION

Supplemental information includes Extended Experimental Procedures, seven supplemental figures, and one supplemental table with this article.

Publisher's Disclaimer: This is a PDF file of an unedited manuscript that has been accepted for publication. As a service to our customers we are providing this early version of the manuscript. The manuscript will undergo copyediting, typesetting, and review of the resulting proof before it is published in its final citable form. Please note that during the production process errors may be discovered which could affect the content, and all legal disclaimers that apply to the journal pertain.

Pacinian corpuscles, Meissner's corpuscles, and Ruffini endings (Johnson, 2001). These tactile end-organs sense a wide range of touch stimuli to generate sensory impulses that enable tactile tasks including the most sophisticated one, tactile discrimination. Merkel discs, also known as Merkel cell-neurite complexes, are formations of Merkel cells and A β -afferent nerve endings in synapse-like structures (Iggo and Muir, 1969; Merkel, 1875). They are highly abundant in fingertips of humans, whisker hair follicles of non-human mammals (Hashimoto, 1972; Merkel, 1875), and other touch-sensitive spots throughout mammalian body (Iggo and Muir, 1969; Munger, 1965). Tactile stimuli to Merkel discs in the skin elicit slowly adapting type I responses (SAI) in A β -afferent fibers (Iggo and Muir, 1969; Johansson and Flanagan, 2009). This tactile-induced SAI response allows fingertips of humans and whiskers of non-human mammals to perform tactile discrimination of an object's shape, curvature, texture, and other physical properties (Carvell and Simons, 1990; Johnson, 2001). Under pathological conditions such as peripheral neuropathy, touch sensation can be either reduced to cause numbness or exaggerated to result in tactile allodynia.

Although Merkel cells were discovered 139 years ago (Merkel, 1875), cellular and molecular mechanisms underlying tactile transduction in Merkel discs remain unclear after over a century studies (Halata et al., 2003). It is also unknown how tactile transduction is further encoded in Merkel discs and how the SAI response in A β -afferent endings is generated. Deletion of Merkel cells from animals chemically (Ikeda et al 1994; Senok et al 1996) or genetically (Maricich et al 2009) results in the loss of SAI response to light touch. However, Merkel cells have not been shown to have any tactile sensitivity in previous studies (Yamashita et al., 1992). In fact, Merkel cells have been believed to be merely supportive tissues for nerve endings' functions (Gottschaldt and Vahle-Hinz, 1981).

Molecular mechanisms underlying the transduction of touch by tactile end-organs are also largely unknown in mammals, while molecules that transduce touch have been identified in sensory neurons of some invertebrates. In *Caenorhabditis elegans*, DEG/ENaC channels transduce touch stimuli to excite touch-sensing neurons (Driscoll and Chalfie, 1991; Huang and Chalfie, 1994). Mammalian homologues to *C. elegans* DEG/ENaC channels are expressed in mammalian sensory neurons (Fricke et al., 2000; Price et al., 2000), but deletion of these channels in mice either does not result in touch defects (Drew et al., 2004) or produces only modest defects (Price et al., 2000). In *Drosophila* larvae, No mechanoreceptor potential C (NOMPC) channels have been shown to be touch transducers and their activation by light touch directly excites *Drosophila* mechanosensory neurons (Yan et al., 2013). Piezo ion channels (Piezo1 and Piezo2) have recently been identified as mechanically activated ion channels (MA) and are expressed in several mammalian tissues (Coste et al., 2010). Piezo2 channels are expressed in dorsal root ganglion (DRG) neurons and have been shown to be involved in mechanotransduction (Coste et al., 2010; Eijkelkamp et al., 2013; Lou et al., 2013). However, studies thus far have not identified whether Piezo2 or any other molecule is used by a tactile end-organ for sensing tactile stimuli in mammals.

In the present study, we set out to answer the questions of whether tactile stimuli are transduced by Merkel cells or by A β -afferent endings in Merkel discs, what molecules are

involved in the tactile transduction in Merkel discs, and how tactile stimuli are encoded by Merkel discs to drive SAI impulses in A β -afferent endings.

RESULTS

Merkel cells *in situ* are excitable cells that fire Ca²⁺-action potentials in a slowly adapting manner

Patch-clamp recording is the most direct way to detect and study mechanotransduction in a cell, but it is technically challenging to apply this technique to intact cells of any tactile end-organ due to tissue barriers. In previous studies, dissociated Merkel cells were patch-clamp recorded but they did not respond to mechanical stimuli (Yamashita et al., 1992). An isolated rat whisker hair follicle preparation was developed for extracellular recordings from whisker afferent bundles but patch-clamp recording has never been performed on Merkel cells in this preparation due to tissue barriers (Baumann et al., 1996). Merkel cells in whisker hair follicles are covered by layers of tough tissues including the follicle capsule, ring sinus tissues, and glassy membranes (Figure 1A). We performed micro-procedures to remove these tissues so that the Merkel cell layer was on the surface of the preparation (Figure 1B and 1C). Merkel cells in our preparation had elongated cell bodies and antenna-like processes (Figure 1C and 1D) similar to their original shapes before removing the tissue barriers. For patch-clamp recordings on Merkel cells, we pre-identified Merkel cells by vital staining with quinacrine (Figure 1C), a fluorescent marker for Merkel cells (Crowe and Whitear, 1978).

The first striking finding was that Merkel cells *in situ* fired multiple action potentials (APs) when they were injected with small depolarizing currents (Figure 1E, 48/48 cells). APs in Merkel cells significantly increased intracellular Ca²⁺ in Merkel cells (Figure 1D and 1F). Our finding that Merkel cells *in situ* fire multiple APs was surprising since cells in the skin have been believed to be not excitable. In dissociated Merkel cells, a previous study observed a single abortive potential (Yamashita et al., 1992). In contrast to Merkel cells *in situ*, non-Merkel cells (quinacrine-negative cells) in whisker hair follicles never fired APs (Figure 1I). Other membrane properties also indicated that Merkel cells are excitable cells (Table S1, Figure 1H). The V-I relationship of Merkel cells (Figure 1H) was strongly rectifying and showed a steep current-potential relationship near resting membrane potentials (~ -60 mV), and a depolarizing current as small as 20 pA could lead to over 40 mV membrane depolarization from resting membrane potentials. This strong membrane response occurred because Merkel cells had extremely high membrane input resistance (over 2 G Ω , Table S1). Under voltage-clamp mode, Merkel cells showed strong voltage-activated outward currents with two kinetic components (Figure S1A–S1C). In contrast, the V-I relationship was nearly linear for non-Merkel cells (Figure 1I and 1J).

Voltage-gated Na⁺ channels drive AP firing in most excitable cells including afferent nerve endings. Interestingly, AP firing in Merkel cells was not affected by tetrodotoxin (TTX), a voltage-gated Na⁺ channel blocker (Figure 2A). However, the AP firing was abolished under a low extracellular Ca²⁺ condition (Figure 2B). Furthermore, the AP firing was abolished by cadmium (Cd²⁺), a voltage-gated Ca²⁺ channel (VGCC) blocker (Figure 2C). The AP firing was also abolished by felodipine, a highly selective blocker of L-type VGCCs

(Figure 2D). These results indicate that the AP firing in Merkel cells *in situ* is driven by Ca^{2+} influx through VGCCs. Voltage-clamp recordings showed that Cd^{2+} -sensitive VGCC currents were expressed in Merkel cells (Figure S1D–S1G), consistent with the presence of VGCCs such as L- and P/Q-types shown in dissociated Merkel cells (Haerberle et al., 2004; Yamashita et al., 1992). The VGCC currents in Merkel cells *in situ* were also sensitive to the block by felodipine (Figure S1H–S1K). When Merkel cells were depolarized over a prolonged period, the Ca^{2+} -AP firing was long-lasting, irregular, and adapted slowly (Figure 2E–2H). Thus, in a Merkel disc, the Merkel cell is an excitable element with the ability to fire Ca^{2+} -APs in a slowly adapting manner.

Merkel cells *in situ* transduce touch stimuli into mechanically activated currents

To test if Merkel cells *in situ* transduce mechanical stimuli, we displaced the Merkel cell layer with a piezo-driven probe at sites distant from the recorded Merkel cells. In this way, the mechanical impact was transmitted across adjacent cells to the recorded Merkel cells (Figure 3A–3C). This indirect stimulation, which was used to mimic naturally occurring touch stimuli, evoked MA currents in Merkel cells (273/273 cells). In a sample of 28 Merkel cells, the mechanotransduction threshold, i.e. the mechanical displacement that just elicited a detectable MA current, was $0.66 \pm 0.05 \mu\text{m}$, and the peak amplitude of the current increased with greater displacement distances (Figure 3D and 3F). Similar to indirect stimulation, directly displacing Merkel cell membranes also evoked MA currents (Figure 3E and 3F) with a mechanotransduction threshold of $0.61 \pm 0.07 \mu\text{m}$. MA currents adapted rapidly, but a small steady-state current component (Figure 3D, 3E, S2A, S2B) with enhanced channel conduction noise (Figure S2A) could be observed. The amplitude of the steady-state current component increased in a displacement-dependent manner, and was $16.4 \pm 1.8 \text{ pA}$ (6.2 to 35.0 pA , $n = 25$) with $4 \mu\text{m}$ displacement (Figure S2B). Merkel cells *in situ* may be necessary for demonstrating the mechanotransduction by Merkel cells since previous studies using dissociated Merkel cells failed to elicit MA currents (Yamashita et al., 1992). Unlike Merkel cells, non-Merkel cells did not show significant responses to displacement stimulation (Figure S2C–S2E).

Mechanotransduction in Merkel cells featured fast kinetic MA currents (Figure 3G). The latency of mechanotransduction had an inverse relationship with the displacement distance (Figure 3H). At a displacement of $3.5 \mu\text{m}$, the mechanotransduction latency was $0.96 \pm 0.06 \text{ ms}$ with indirect stimulation and $0.51 \pm 0.03 \text{ ms}$ with direct displacement of Merkel cell membranes (Figure 3H). The short latency of mechanotransduction suggests a direct mechanical gating. MA currents rose faster with increasing displacement distances (Figure 3I). The currents decayed mono-exponentially with time constant of $\sim 6 \text{ ms}$ (Figure 3J), almost identical to the decay kinetics of recently cloned Piezo2 channels (Coste et al., 2010).

We determined Merkel cell MA channel ion permeability by measuring the MA current reversal potentials under different ionic conditions (Figure 3K–3N). I-V relationships of MA currents under normal recording conditions (Figure 3K), extracellular Ca^{2+} and intracellular Cs^+ only ($[\text{Ca}^{2+}]_{\text{out}}/[\text{Cs}^+]_{\text{in}}$) (Figure 3L), $[\text{Na}^+]_{\text{out}}/[\text{Cs}^+]_{\text{in}}$ and $[\text{Na}^+]_{\text{out}}/[\text{K}^+]_{\text{in}}$ conditions (Figure 3M) all yielded reversal potentials near 0 mV . Calculated ion permeability ratios showed that MA channels in Merkel cells are almost equally permeable to Na^+ , K^+ , Cs^+ and

Ca²⁺ (Figure 3N). Thus, Merkel cell MA channels are Ca²⁺-permeable non-selective cation channels.

Mechanotransduction in Merkel cells is mediated by Piezo2 ion channels

We harvested Merkel cells (quinacrine-stained cells) and non-Merkel cells (quinacrine-negative cells) separately by aspirating individual cells into electrode pipettes and then examined Piezo2 mRNA expression in them. Piezo2 mRNA was detected in Merkel cells but not in non-Merkel cells (Figure 4A). We conducted pharmacological tests on MA currents in Merkel cells *in situ*. Merkel cell MA currents were inhibited by gadolinium (Gd³⁺) (Figure 4B) and ruthenium red (RR) (Figure 4C), two compounds that blocked Piezo2 channels in heterologous expression systems (Coste et al., 2010). The degree of inhibition by the two blockers on Merkel cell MA currents (Figure 4B and 4C) was comparable to their inhibition of Piezo2-mediated currents in heterologous expression systems (Coste et al., 2010). We tested Merkel cell MA currents with an antibody against an intracellular segment of Piezo2 (Piezo2Ab). Merkel cell MA currents were significantly reduced by the intracellular application of the Piezo2Ab when compared with a control group without Piezo2Ab (Figure 4D and 4E). The inhibition by Piezo2Ab was abolished in the presence of a blocking peptide for the antibody (Piezo2Ab+BP, Figure 4D and 4E) and was also abolished when the antibody was thermally inactivated (Figure S3B). The inhibition by Piezo2Ab was also evidenced with normalized currents, which showed the reduction of MA currents 10 min after establishing the whole-cell mode when the Piezo2Ab was present in the internal recording solution (Figure S3A and S3B). Similar to Merkel cell MA currents, the rapidly adapting MA currents (McCarter et al., 1999) mediated by Piezo2 in DRG neurons (Coste et al., 2010) were inhibited by the intracellular application of Piezo2Ab (Figure S3C and S3D). On the other hand, MA currents evoked from N2A cells, which were known to be mediated by Piezo1 channels (Coste et al., 2010), were not significantly affected by the Piezo2Ab (Figure S3E and S3F). Voltage-activated currents and AP firing in Merkel cells were also not significantly affected by the Piezo2Ab (Figure S3G–S3J).

We injected Piezo2 shRNA lentiviral particles into whisker hair follicles (Figure 5A) to knock down Piezo2. The solution injected into a whisker follicle stayed inside the follicle because of follicle capsule barrier (Figure 5A). As indicated by GFP expression mediated by GFP lentiviral particles, lentiviral particle-mediated gene expression occurred preferentially in the initial and enlargement segments (Figure S4A), the two sites where Merkel cells are located in a whisker hair follicle (Ebara et al., 2002). Most Merkel cells (67.5%) were GFP-positive and most GFP-positive cells (68.0%) were Merkel cells (Figure 5B and 5C) in the enlargement segment of whisker hair follicles 6–13 days after intra-follicle injections. GFP lentiviral particles injected into whisker hair follicles did not result in detectable GFP expression in ipsilateral whisker afferents (Figure S4C and S4D), consistent with the lack of retrograde transport of lentiviral particles by afferent fibers (Yu et al., 2011). Incorporation of lentiviral vector construct into genomic DNA of host cells is required for and precedes lentiviral particle-mediated shRNA synthesis and subsequent gene knockdown. We found that the woodchuck hepatitis posttranscriptional regulatory element (WPRE) (Zufferey et al., 1999), an essential part of lentiviral vector construct for gene knockdown, was incorporated

into the genomic DNA of the cells in whisker hair follicles but not in the ipsilateral trigeminal afferents (Figure S4I–S4K). We measured relative Piezo2 mRNAs by qPCR. In comparison with the control group with scrambled shRNA, injection of Piezo2 shRNA lentiviral particles into whisker hair follicles resulted in ~50% reduction of Piezo2 mRNA in the enlargement segments of whisker hair follicles (Figure 5D, Figure S5A–S5C).

We examined Merkel cell MA currents after intra-follicle injections of Piezo2 shRNA lentiviral particles (Figure 5E). While injection of scrambled shRNA lentiviral particles had no effect on MA currents in Merkel cells when compared with un-injected group, injection of Piezo2 shRNA lentiviral particles resulted in a significant reduction of MA currents in comparison with the injection of scrambled shRNA lentiviral particles (Figure 5E and 5F). Merkel cells had a mechanotransduction threshold $\approx 1.5 \mu\text{m}$ in follicles not injected or injected with scrambled shRNA lentiviral particles (Figure 5G), but ~50% of Merkel cells had mechanotransduction thresholds of $\approx 2.0 \mu\text{m}$ after Piezo2 shRNA lentiviral particle injections (Figure 5G). Overall, the mechanotransduction threshold in the Piezo2 shRNA group was increased by ~3 fold when compared with the scrambled shRNA group (Figure 5H). In whisker hair follicles injected with Piezo2 shRNA lentiviral particles, the Merkel cells with high mechanotransduction threshold ($\approx 2.0 \mu\text{m}$) had smaller MA currents in comparison with those Merkel cells with low mechanotransduction threshold ($\approx 1.5 \mu\text{m}$) (Figure 5I). While Piezo2 knockdown significantly reduced MA currents in Merkel cells, it did not affect voltage-activated currents (Figure S5D and S5E) and electrically-evoked AP firing in Merkel cells (Figure S5F and S5G). Intra-follicle application of Piezo1 shRNA lentiviral particles did not affect MA currents in Merkel cells (Figure S5H and S5I).

Natural tactile stimuli are transduced by Merkel cells and encoded as action potentials in Merkel cells

Can Merkel cell MA channels transduce a natural tactile stimulus? To address this issue, we tested if hair movement could induce the characteristic MA currents in Merkel cells because hair movement is the natural tactile stimulus. Similar to indirect and direct displacement stimulation of Merkel cells, a small hair movement elicited MA currents in Merkel cells and the mechanotransduction threshold was $1.3 \pm 0.2 \mu\text{m}$ (Figure 6A–6C). At $4 \mu\text{m}$ hair movement, MA currents were $\sim 60 \text{ pA}$, ~ 2 fold of rheobase for firing APs in Merkel cells (Figure 6C). Merkel cell MA currents induced by hair movement were also characteristically transient (Figure 6B) with kinetics identical to Merkel cell MA currents that were induced by displacement stimulation of Merkel cells. Thus, natural tactile stimulation by gentle hair movement can be transduced into MA currents in Merkel cells *in situ*.

We then asked if hair movement-induced tactile transduction in Merkel cells can depolarize the membrane sufficiently to generate AP discharges, i.e. encoding the tactile stimuli into Merkel cell impulses. Under the cell-attached recording mode, AP spike currents in Merkel cells were induced by hair movement (Figure 6D–6F). Some Merkel cells fired a single spike following a single supra-threshold stimulus (Figure 6D and 6F). Other Merkel cells showed graded responses with multiple spikes when hair displacement distances were increased (Figure 6E and 6F). Similar to tactile stimulation by hair movement, AP discharges in Merkel cells could also be induced by indirect displacement stimulation to

Merkel cells when recorded under the cell-attached recording mode (Figure 6G, 6H and 6J). Some Merkel cells fired a single spike following a single supra-threshold displacement step (Figure 6G and 6J). Other Merkel cells showed graded responses with multiple spikes when displacement distances were increased (Figure 6H and 6J). After breaking into the whole-cell mode, both Merkel cell APs (Figure 6I top panel) and MA currents (Figure 6I bottom panel) could be elicited in the same Merkel cells following indirect displacement stimulation to the Merkel cells. These results indicate that in Merkel discs the Piezo2-mediated tactile transduction in Merkel cells is encoded into AP firing in Merkel cells.

Ca²⁺-action potentials and Piezo2 channels in Merkel cells are required to drive SAI responses in A β -afferent fibers

Is the tactile encoding by Ca²⁺-APs in Merkel cells essential for generating SAI impulses in A β -afferent nerve endings during hair movement? To address this issue, we used whisker hair follicles that had attached whisker afferent bundles and recorded afferent impulses with suction electrodes (Figure 7A). Low micrometer hair movement resulted in SAI impulses recorded from whisker afferent fibers (Figure 7B). TTX, which is able to block A β -afferent conduction due to its inhibition of Na⁺-APs, abolished SAI impulses in whisker afferents (Figure 7B). Bath application of Cd²⁺, which selectively abolished Ca²⁺-APs in Merkel cells, also inhibited SAI responses (Figure 7C and 7D). Cd²⁺ almost completely abolished the static phase of SAI impulses and also largely inhibited the dynamic phase of SAI impulses in whisker afferents (Figure 7C and 7D). Cd²⁺ did not reduce excitability of large-sized trigeminal afferent neurons (Figure S6A–S6C). Focal application of Cd²⁺ onto whisker afferent fibers did not produce conduction block of SAI impulses (Figure S6D–S6F). Cd²⁺ also had no effect on MA currents in either Merkel cells *in situ* or cultured trigeminal afferent neurons (Figure S6I and S6J). These results suggest that Ca²⁺-APs in Merkel cells are required to drive SAI impulses.

The L-type VGCC inhibitor verapamil was previously reported to inhibit SAI impulses (Ogawa and Yamashita, 1988) and we reproduced this result (Figure S7A and S7B). However, this effect could not be simply attributed to the inhibition of Ca²⁺-APs in Merkel cells since verapamil also directly blocked whisker afferent conduction (Figure S7C–S7F) probably due to its non-specific effect on K⁺ conductance (Hogg et al., 1999). Therefore, we tested felodipine, another L-type VGCC blocker with high selectivity, on SAI responses induced by whisker hair movement. Felodipine significantly inhibited SAI responses when it was applied onto whisker hair follicles through bath application (Figure 7E and 7F). On the other hand, focal application of felodipine onto whisker afferent fibers did not produce conduction block of SAI responses (Figure S7G and S7H). Felodipine also had no effect on Merkel cell MA currents (Figure S7I and S7J). Since Merkel cells also express N- and P/Q-type of VGCCs (Haeberle et al., 2004), we tested ω -conotoxin MVIIC, a selective blocker of these VGCCs. We found that ω -conotoxin MVIIC also significantly inhibited SAI responses (Figure 7G and 7H). Thus, in Merkel discs, the slowly adapting Ca²⁺-APs in Merkel cells are required to drive SAI response in A β -afferent nerve endings during hair movement.

Is Piezo2 in whisker hair follicles essential for driving SAI impulses during whisker hair movement? To answer this question, we examined SAI responses after intra-follicle injections of Piezo2 shRNA lentiviral particles to knockdown Piezo2. In comparison with the control group injected with scrambled shRNA lentiviral particles, SAI responses were significantly reduced 10 days after intra-follicle injections of Piezo2 shRNA lentiviral particles (Figure 7I and 7J). Since Piezo2 in Merkel cells is the primary target of Piezo2 shRNA using our knockdown approach (Figure 5A–5C, Figure S4) and non-Merkel cells has no detectible MA currents (Figure S2C–S2E), our results indicate that Piezo2 in Merkel cells is the primary mechanical transducer that drives SAI responses during whisker hair movement.

Ca²⁺-action potentials and Piezo2 in Merkel cells are required for behavioral whisker tactile responses

We performed the whisker tactile test to determine if Piezo2 and Ca²⁺-APs in Merkel cells are required for behavioral whisker tactile responses (Figure 7K–7M). Innate tactile responses to gently touching whisker hairs induced head reorientation in some animals but this whisker tactile behavior could not be quantitatively measured because of the lack of consistency and rapid adaptation. To overcome this problem, we subcutaneously injected a small amount of capsaicin into the facial areas of testing rats prior to behavioral tests. Capsaicin is known to induce central sensitization which can amplify behavioral readouts, and it does not alter the conduction of tactile signals by A β -afferent fibers (Sang et al., 1996; Torebjork et al., 1992). We examined behavioral whisker tactile responses in capsaicin-treated animals by gently touching whisker hairs with a thin filament (Figure 7K). The filament movement towards the whisker was controlled at a low speed (< 3 mm/s) so that the potential involvement of the rapidly adapting tactile receptors (e.g. lanceolate endings) in the whisker hair follicles could be minimized (Shoykhet et al., 2000). The behavior tactile sensitivity, measured by nocifensive reactions to the tactile stimuli, was high in the capsaicin-injected rats without other treatments (Figure 7L).

We injected the test drugs or saline into whisker hair follicles and then performed the whisker tactile test on the associated whiskers. The intra-follicle drug application is essential for delivering testing drugs to Merkel discs within a whisker hair follicle because a whisker hair follicle in the skin is insulated by its follicle capsule. Intra-follicle saline application had no effect on the whisker tactile-induced nocifensive responses (Figure 7L). Intra-follicle application of TTX, which would block AP firing on afferent nerve endings within the whisker hair follicles, suppressed the whisker tactile-induced nocifensive responses (Figure 7L). Intra-follicle application of Cd²⁺, felodipine, or ω -conotoxin MVIIC, which would abolish Ca²⁺-AP firing in Merkel cells (see Figure 2D) and suppress SAI responses (see Figure 7C–7H), also significantly suppressed the whisker tactile-induced nocifensive responses (Figure 7L).

We injected Piezo2 shRNA lentiviral particles into whisker hair follicles and tested if Piezo2 knockdown could suppress whisker tactile-induced nocifensive behavioral responses (Figure 7M). The whisker tactile-induced nocifensive responses were significantly reduced 7 or more days after the injection of Piezo2 shRNA lentiviral particles (Figure 7M). However,

injection of scrambled shRNA lentiviral particles into whisker hair follicles did not result in any change of the whisker tactile-induced nocifensive responses (Figure 7M). These results showed the involvement of Piezo2 in behavioral tactile responses.

DISCUSSION

The study of mechanisms underlying mechanotransduction has recently advanced from invertebrates (Chalfie and Au, 1989; Kernan et al., 1994; Yan et al., 2013) to mammals (Coste et al., 2010). We show that Merkel cells, rather than their associated A β -afferent nerve endings, are primary sites of both tactile transduction and encoding. This cellular mechanism is distinct from those in invertebrates, where tactile stimuli are directly transduced by touch-sensing afferent nerves. In mammals, all other somatosensory stimuli are also directly transduced by afferent nerve endings (Basbaum et al., 2009). However, specialized sensory organs including the ear and the eye do not use afferent nerves to transduce stimuli. Instead, hair cells in the ear and photoreceptor cells in the eye are evolved into specialized transducer cells (Burns and Arshavsky, 2005). Thus, the Merkel cell is another class of specialized transducer cell that has evolved for sensing light touch to enable sensory tasks including tactile discrimination.

We have elucidated the molecular mechanism of tactile transduction in Merkel cells by identifying Piezo2 ion channels as their mechanotransducers. This finding is somewhat unexpected because Piezo2 was reported to have low expression in the skin (Coste et al., 2010). We show that Piezo2 is expressed in Merkel cells but not in non-Merkel cells in whisker hair follicles. Since the numbers of Merkel cells are small in the skin, it explains why Piezo2 expression is low in the skin. Consistently, we showed that MA currents could be elicited in Merkel cells but not in non-Merkel cells. A number of ion channels including DEG/ENaC channels, K⁺ channels, TRP channels have been proposed to be candidate mechanotransducers (Chalfie, 2009), but our MA channels in Merkel cells have properties distinct from those candidates. On the other hand, we showed that electrophysiological and pharmacological properties of MA currents in Merkel cells are almost identical to Piezo2-mediated MA currents in heterologous expression system (Coste et al., 2010). Furthermore, MA currents in Merkel cells are reduced by Piezo2 knockdown and by a Piezo2 antibody. These findings together indicate that Piezo2 is the mechanotransducer in Merkel cells.

In our study MA current in Merkel cells adapted rapidly, raising a question whether Piezo2 activation can lead Merkel cells to fire slowly adapting APs to encode sustained tactile stimuli. In addition to the rapidly adapting component, we show that MA current in Merkel cells has a long-lasting steady-state current component with the amplitude up to 35 pA at 4 μ m displacement. This small current could depolarize Merkel cell membrane sufficiently to fire APs because Merkel cells *in situ* have extremely high membrane input resistances (2.1 G Ω on average). It is likely that the steady-state current components in Merkel cells would maintain sufficient membrane depolarization to sustain AP firing.

SAI responses recorded in A β -afferent fibers are critical for tactile discrimination (Blake et al., 1997; Johansson and Flanagan, 2009; Johnson, 2001). We show that injection of Piezo2 shRNA lentiviral particles, which significantly reduced Piezo2-mediated MA currents in

Merkel cells, also significantly reduced SAI responses. This result indicates that Piezo2 in Merkel cells play a major role in tactile transduction that subsequently drives SAI responses during whisker hair movement. We show that Merkel cells fire Ca^{2+} -APs in a long lasting, slowly adapting manner. The slowly adapting Ca^{2+} -APs following Piezo2-mediated tactile transduction in Merkel cells may be an underlying mechanism that drives SAI response in $\text{A}\beta$ -afferent fibers. This is supported by our finding that the static phase of SAI response in whisker afferent fibers could be eliminated and the dynamic phase of SAI response in whisker afferent fibers also largely abolished when Ca^{2+} -AP firing was prevented in Merkel cells. The small portion of the dynamic phase that was independent of Ca^{2+} -APs shown in this study might be due to a direct Ca^{2+} entry through Piezo2 channels during their initial activation. Some Piezo2-expressing afferent fibers (Coste et al., 2010) that innervate hair follicles (Lou et al., 2013) may also contribute to the dynamic phase of SAI response. We show that an individual Merkel cell fires slowly adapting Ca^{2+} -APs at ~1.5 Hz in the static phase but SAI impulses in whisker afferent bundle are at much higher frequency in the static phase. Ca^{2+} -APs in many individual Merkel cells may contribute to the high frequency of SAI impulses in whisker afferent fibers.

The requirement of slowly adapting Ca^{2+} -APs in Merkel cells for driving SAI impulses in $\text{A}\beta$ -afferent fibers shown in our study suggests that excitatory signals in Merkel cells are transmitted to $\text{A}\beta$ -afferent nerve endings. Merkel cells and $\text{A}\beta$ -afferent nerve endings form synaptic-like structures in Merkel discs (Iggo and Muir, 1969). Merkel cells are packed with neurotransmitter-containing vesicles (Munger, 1965) and also have other neuronal synaptic release machinery (Haeberle et al., 2004). Furthermore, a number of substances such as VIP, substance P, enkephalin, CGRP, 5-HT have been identified in the vesicles of Merkel cells (English et al., 1992; Garcia-Caballero et al., 1989; Tachibana and Nawa, 2005; Zaccone, 1986; Zaccone et al., 1995). Thus, tactile stimulation-induced Ca^{2+} -APs may trigger transmitter release from Merkel cells onto postsynaptic $\text{A}\beta$ -afferent endings to subsequently induce $\text{A}\beta$ -afferent SAI impulses.

Piezo2 and Ca^{2+} -APs in Merkel cells are required for behavioral tactile responses since Piezo2 knockdown in whisker hair follicles or selective inhibition of Ca^{2+} -APs impairs behavioral tactile responses. This behavioral outcome is consistent with our electrophysiological results showing that MA currents in Merkel cells were largely reduced by Piezo2 knockdown and that SAI responses were suppressed when Piezo2 was knocked down or when Ca^{2+} -APs in Merkel cells were abolished. The behavioral outcomes following intra-follicle injection of Piezo2 shRNA lentiviral particles can be attributed primarily to the knockdown of Piezo2 in Merkel cells. This is because Piezo2 in Merkel cells is the primary target for lentiviral particle-mediated Piezo2 knockdown in our study and non-Merkel cells had no detectible MA currents. We administered TRPV1 agonist capsaicin (Caterina et al., 1997) prior to behavioral tests in order to produce reliable tactile responses. Capsaicin sensitizes peripheral nociceptive afferent nerve endings to induce thermal and mechanical hyperalgesia (Sang et al., 1996). However, the capsaicin-sensitized nociceptive afferent endings themselves could not respond to tactile stimuli (Sang et al., 1996; Torebjork et al., 1992). Therefore, capsaicin-sensitive nociceptive afferent endings cannot be the tactile transduction/conduction pathways in our behavioral study. Capsaicin also induces central sensitization such that tactile signals conducted by $\text{A}\beta$ -afferent fiber are

misinterpreted in the CNS as painful stimuli to result in tactile allodynia (Sang et al., 1996; Torebjork et al., 1992). Since A β -afferent fibers are involved in conduction of tactile signals in capsaicin-treated animals (Sang et al., 1996; Torebjork et al., 1992), we interpret our behavioral outcomes to mean that tactile stimuli to whisker hairs are primarily transduced by Piezo2 and encoded by Ca²⁺-APs in Merkel cells, and then transmitted to A β -afferent fibers to lead to behavioral tactile responses.

Using mice whose Merkel cells are genetically deleted, recent studies have shown that Merkel cells are essential in light touch responses (Maricich et al., 2009) and texture discrimination involving glabrous skin (Maricich et al., 2012). These studies highlight the importance of the basic mechanisms underlying the tactile transduction and encoding in Merkel discs shown by our current work. Interestingly, whisker-mediated texture discrimination or whisker brushing-induced reflex responses were not found to be different between normal mice and Merkel cell-deletion mice (Maricich et al., 2012). This may be related in part to the presence of other tactile-end organs such as rapidly adapting lanceolate endings in whisker hair follicles (Ebara et al., 2002) that may still perform some tactile tasks. SAI responses are essential for high spatial resolution tactile discrimination, and rapidly adapting responses are also involved in tactile discrimination but with a low spatial resolution (Blake et al., 1997; Johnson, 2001).

The mechanisms underlying the transduction and encoding of tactile stimuli by Merkel discs shown in our study represent fundamental signaling processes for Merkel discs that are not only located in whisker hair follicles but also in other touch sensitive spots (e.g. touch domes) throughout the body. The biological processes in Merkel discs described here should help further understanding of tactile responses including the most sophisticated one, tactile discrimination. Our findings may also have clinical implications since tactile dysfunction including reduced tactile sensitivity or tactile allodynia are commonly seen in patients with diabetes, chemotherapy, and inflammation.

EXPERIMENTAL PROCEDURES

All experimental procedures performed on rats were approved by the University of Cincinnati Institutional Animal Care and Use Committees.

Merkel cell *in situ* preparations

Whisker hair follicles were dissected out from rat whisker pads and the capsule of each follicle was removed. The follicles with their hair shafts were then fixed in a recording chamber and submerged in a Krebs solution. The follicles were exposed to a gentle enzyme treatment, and ring sinus cells and the glassy membranes were then peeled off. Merkel cells were vital-stained by quinacrine and pre-identified using a fluorescent imaging system.

Patch-clamp recordings

Whole-cell MA currents were recorded from Merkel cells under the voltage-clamp mode. AP firing in response to membrane depolarization was recorded under the whole-cell current-clamp mode. To determine AP firing in Merkel cells following mechanical stimulation, AP spike currents were recorded under the cell-attached recording mode.

Whisker afferent fiber recordings

Hair follicles with attached whisker afferent fiber bundles were fixed in a recording chamber. The whisker hair was attached to a piezo device for hair movement. The whisker afferent nerve bundle was sucked into a tightly fitted recording electrode to record compound APs.

Mechanical Stimulation

Mechanical stimulation was applied either by displacing hair follicle tissues or by hair movement. For displacing hair follicle tissues, a fire-polished blunted glass probe was used. The stepwise forward movement of the probe was delivered by a piezo device. For hair movement, the hair shaft was deflected by a piezo with a step movement that had a short ramp before reaching the static phase of the step.

Pharmacology

Merkel cell APs were tested with TTX, Cd²⁺, felodipine, or low Ca²⁺. Merkel cell MA currents were tested with Gd³⁺, RR, Cd²⁺ or a Piezo2 antibody. The antibody was included in the recording electrode internal solution. SAI responses recorded from whisker afferent fibers were tested with TTX, Cd²⁺, felodipine, and ω -conotoxin MVIIC.

Piezo2 knockdown

Piezo2- or scrambled shRNA lentiviral particles were injected into whisker hair follicles. The injected follicles were harvested 6–11 days later. Patch-clamp recordings of MA currents from Merkel cells were then performed.

RT-PCR and qPCR

PCR primers were: Piezo1 forward ACAGGTCGCCTGCTTCGTGC, reverse TGCCACCAGCACTCCCAGGT; Piezo2 forward TTCGGAAGTGGTGTGCGGGC, and reverse GTAAGCGGTGCGATGCGGT.

Behavioral tactile sensitivity of whisker hairs

Testing drugs and Piezo2 shRNA lentiviral particles were injected into hair follicles. The whisker tactile test was performed by displacing whisker hairs for ~2 mm in caudal-rostral direction using a thin plastic filament.

Data Analysis

Data are presented as mean \pm SEM. Statistical significance was evaluated using Student's t-test for two groups, one-way or two-way ANOVA with Bonferroni post-hoc tests for multiple groups, * p<0.05, ** p<0.01, and *** p<0.001.

Supplementary Material

Refer to Web version on PubMed Central for supplementary material.

Acknowledgments

We thank Drs. A. MacDermott, M. Salter, J. Strong and M. Baccei for comments on an earlier version of this manuscript. This work was supported by NIH grants DE018661 and DE023090 to J.G.G, a travel fellowship to R.I. from The Mochida Memorial Foundation for Medical and Pharmaceutical Research of Japan, a scholarship to Z.J. from NSF of China (NSFC, 31000376).

References

- Basbaum AI, Bautista DM, Scherrer G, Julius D. Cellular and molecular mechanisms of pain. *Cell*. 2009; 139:267–284. [PubMed: 19837031]
- Baumann KI, Chan E, Halata Z, Senok SS, Yung WH. An isolated rat vibrissal preparation with stable responses of slowly adapting mechanoreceptors. *Neurosci Lett*. 1996; 213:1–4. [PubMed: 8844698]
- Blake DT, Johnson KO, Hsiao SS. Monkey cutaneous SAI and RA responses to raised and depressed scanned patterns: effects of width, height, orientation, and a raised surround. *J Neurophysiol*. 1997; 78:2503–2517. [PubMed: 9356401]
- Burns ME, Arshavsky VY. Beyond counting photons: trials and trends in vertebrate visual transduction. *Neuron*. 2005; 48:387–401. [PubMed: 16269358]
- Carvell GE, Simons DJ. Biometric analyses of vibrissal tactile discrimination in the rat. *J Neurosci*. 1990; 10:2638–2648. [PubMed: 2388081]
- Caterina MJ, Schumacher MA, Tominaga M, Rosen TA, Levine JD, Julius D. The capsaicin receptor: a heat-activated ion channel in the pain pathway. *Nature*. 1997; 389:816–824. [PubMed: 9349813]
- Chalfie M. Neurosensory mechanotransduction. *Nat Rev Mol Cell Biol*. 2009; 10:44–52. [PubMed: 19197331]
- Chalfie M, Au M. Genetic control of differentiation of the *Caenorhabditis elegans* touch receptor neurons. *Science*. 1989; 243:1027–1033. [PubMed: 2646709]
- Coste B, Mathur J, Schmidt M, Earley TJ, Ranade S, Petrus MJ, Dubin AE, Patapoutian A. Piezo1 and Piezo2 Are Essential Components of Distinct Mechanically Activated Cation Channels. *Science*. 2010; 330:55–60. [PubMed: 20813920]
- Crowe R, Whitear M. Quinacrine fluorescence of Merkel cells in *Xenopus laevis*. *Cell Tissue Res*. 1978; 190:273–283. [PubMed: 79446]
- Drew LJ, Rohrer DK, Price MP, Blaver KE, Cockayne DA, Cesare P, Wood JN. Acid-sensing ion channels ASIC2 and ASIC3 do not contribute to mechanically activated currents in mammalian sensory neurones. *J Physiol*. 2004; 556:691–710. [PubMed: 14990679]
- Driscoll M, Chalfie M. The *mec-4* gene is a member of a family of *Caenorhabditis elegans* genes that can mutate to induce neuronal degeneration. *Nature*. 1991; 349:588–593. [PubMed: 1672038]
- Ebara S, Kumamoto K, Matsuura T, Mazurkiewicz JE, Rice FL. Similarities and differences in the innervation of mystacial vibrissal follicle-sinus complexes in the rat and cat: a confocal microscopic study. *J Comp Neurol*. 2002; 449:103–119. [PubMed: 12115682]
- Eijkelkamp N, Linley JE, Torres JM, Bee L, Dickenson AH, Gringhuis M, Minett MS, Hong GS, Lee E, Oh U, et al. A role for Piezo2 in EPAC1-dependent mechanical allodynia. *Nat Commun*. 2013; 4:1682. [PubMed: 23575686]
- English KB, Wang ZZ, Stayner N, Stensaas LJ, Martin H, Tuckett RP. Serotonin-like immunoreactivity in Merkel cells and their afferent neurons in touch domes from the hairy skin of rats. *Anat Rec*. 1992; 232:112–120. [PubMed: 1536455]
- Fricke B, Lints R, Stewart G, Drummond H, Dodt G, Driscoll M, von Düring M. Epithelial Na⁺ channels and stomatin are expressed in rat trigeminal mechanosensory neurons. *Cell Tissue Res*. 2000; 299:327–334. [PubMed: 10772247]
- García-Caballero T, Gallego R, Roson E, Basanta D, Morel G, Beiras A. Localization of serotonin-like immunoreactivity in the Merkel cells of pig snout skin. *Anat Rec*. 1989; 225:267–271. [PubMed: 2589641]
- Gottschaldt KM, Vahle-Hinz C. Merkel cell receptors: structure and transducer function. *Science*. 1981; 214:183–186. [PubMed: 7280690]

- Haerberle H, Fujiwara M, Chuang J, Medina MM, Panditrao MV, Bechstet S, Howard J, Lumpkin EA. Molecular profiling reveals synaptic release machinery in Merkel cells. *Proc Natl Acad Sci U S A*. 2004; 101:14503–14508. [PubMed: 15448211]
- Halata Z, Grim M, Bauman KI. Friedrich Sigmund Merkel and his “Merkel cell”, morphology, development, and physiology: review and new results. *Anat Rec A Discov Mol Cell Evol Biol*. 2003; 271:225–239. [PubMed: 12552639]
- Hashimoto K. The ultrastructure of the skin of human embryos. X. Merkel tactile cells in the finger and nail. *J Anat*. 1972; 111:99–120. [PubMed: 5016952]
- Hogg RC, Trequatrin C, Catacuzzeno L, Petris A, Franciolini F, Adams DJ. Mechanisms of verapamil inhibition of action potential firing in rat intracardiac ganglion neurons. *J Pharmacol Exp Ther*. 1999; 289:1502–1508. [PubMed: 10336545]
- Huang M, Chalfie M. Gene interactions affecting mechanosensory transduction in *Caenorhabditis elegans*. *Nature*. 1994; 367:467–470. [PubMed: 7509039]
- Iggo A, Muir AR. The structure and function of a slowly adapting touch corpuscle in hairy skin. *J Physiol*. 1969; 200:763–796. [PubMed: 4974746]
- Johansson RS, Flanagan JR. Coding and use of tactile signals from the fingertips in object manipulation tasks. *Nat Rev Neurosci*. 2009; 10:345–359. [PubMed: 19352402]
- Johnson KO. The roles and functions of cutaneous mechanoreceptors. *Curr Opin Neurobiol*. 2001; 11:455–461. [PubMed: 11502392]
- Kernan M, Cowan D, Zuker C. Genetic dissection of mechanosensory transduction: mechanoreception-defective mutations of *Drosophila*. *Neuron*. 1994; 12:1195–1206. [PubMed: 8011334]
- Lou S, Duan B, Vong L, Lowell BB, Ma Q. Runx1 controls terminal morphology and mechanosensitivity of VGLUT3-expressing C-mechanoreceptors. *J Neurosci*. 2013; 33:870–882. [PubMed: 23325226]
- Maricich SM, Morrison KM, Mathes EL, Brewer BM. Rodents rely on Merkel cells for texture discrimination tasks. *J Neurosci*. 2012; 32:3296–3300. [PubMed: 22399751]
- Maricich SM, Wellnitz SA, Nelson AM, Lesniak DR, Gerling GJ, Lumpkin EA, Zoghbi HY. Merkel cells are essential for light-touch responses. *Science*. 2009; 324:1580–1582. [PubMed: 19541997]
- McCarter GC, Reichling DB, Levine JD. Mechanical transduction by rat dorsal root ganglion neurons in vitro. *Neurosci Lett*. 1999; 273:179–182. [PubMed: 10515188]
- Merkel F. Tastzellen und Tastkoerperchen bei den Hausthieren und beim Menschen. *Arch Mikrosk Anat*. 1875; 11:636–652.
- Munger BL. The intraepidermal innervation of the snout skin of the opossum. A light and electron microscope study, with observations on the nature of Merkel’s Tastzellen. *J Cell Biol*. 1965; 26:79–97. [PubMed: 5859024]
- ogawa H, Yamashita Y. Mechano-electric transduction in the slowly adapting cutaneous afferent units of frogs. *Prog Brain Res*. 1988; 74:63–68. [PubMed: 3263669]
- Price MP, Lewin GR, McIlwrath SL, Cheng C, Xie J, Heppenstall PA, Stucky CL, Mannsfeldt AG, Brennan TJ, Drummond HA, et al. The mammalian sodium channel BNC1 is required for normal touch sensation. *Nature*. 2000; 407:1007–1011. [PubMed: 11069180]
- Sang CN, Gracely RH, Max MB, Bennett GJ. Capsaicin-evoked mechanical allodynia and hyperalgesia cross nerve territories. Evidence for a central mechanism. *Anesthesiology*. 1996; 85:491–496. [PubMed: 8853078]
- Shoykhet M, Doherty D, Simons DJ. Coding of deflection velocity and amplitude by whisker primary afferent neurons: implications for higher level processing. *Somatosens Mot Res*. 2000; 17:171–180. [PubMed: 10895887]
- Tachibana T, Nawa T. Immunohistochemical reactions of receptors to met-enkephalin, VIP, substance P, and CGRP located on Merkel cells in the rat sinus hair follicle. *Arch Histol Cytol*. 2005; 68:383–391. [PubMed: 16505584]
- Torebjork HE, Lundberg LE, LaMotte RH. Central changes in processing of mechanoreceptive input in capsaicin-induced secondary hyperalgesia in humans. *J Physiol*. 1992; 448:765–780. [PubMed: 1593489]

- Yamashita Y, Akaike N, Wakamori M, Ikeda I, Ogawa H. Voltage-dependent currents in isolated single Merkel cells of rats. *J Physiol.* 1992; 450:143–162. [PubMed: 1331421]
- Yan Z, Zhang W, He Y, Gorczyca D, Xiang Y, Cheng LE, Meltzer S, Jan LY, Jan YN. *Drosophila* NOMPC is a mechanotransduction channel subunit for gentle-touch sensation. *Nature.* 2013; 493:221–225. [PubMed: 23222543]
- Yu H, Fischer G, Jia G, Reiser J, Park F, Hogan QH. Lentiviral gene transfer into the dorsal root ganglion of adult rats. *Mol Pain.* 2011; 7:63. [PubMed: 21861915]
- Zaccone G. Neuron-specific enolase and serotonin in the Merkel cells of conger-eel (*Conger conger*) epidermis. An immunohistochemical study. *Histochemistry.* 1986; 85:29–34. [PubMed: 3525473]
- Zaccone G, Fasulo S, Ainis L, Mauceri A, Licata A, Lauriano ER. Enkephalin immunoreactivity in the paraneurons of the tiger salamander (*Ambystoma tigrinum*) tongue. *Neuropeptides.* 1995; 28:257–260. [PubMed: 7603585]
- Zufferey R, Donello JE, Trono D, Hope TJ. Woodchuck hepatitis virus posttranscriptional regulatory element enhances expression of transgenes delivered by retroviral vectors. *J Virol.* 1999; 73:2886–2892. [PubMed: 10074136]

Highlight

Merkel cells are primary sites of tactile transduction and encoding

Piezo2 ion channels mediate tactile transduction in Merkel cells

Tactile transduction is encoded as Ca^{2+} -action potentials in Merkel cells

Merkel cell Ca^{2+} -action potentials drive slowly adapting $\text{A}\beta$ -afferent impulses

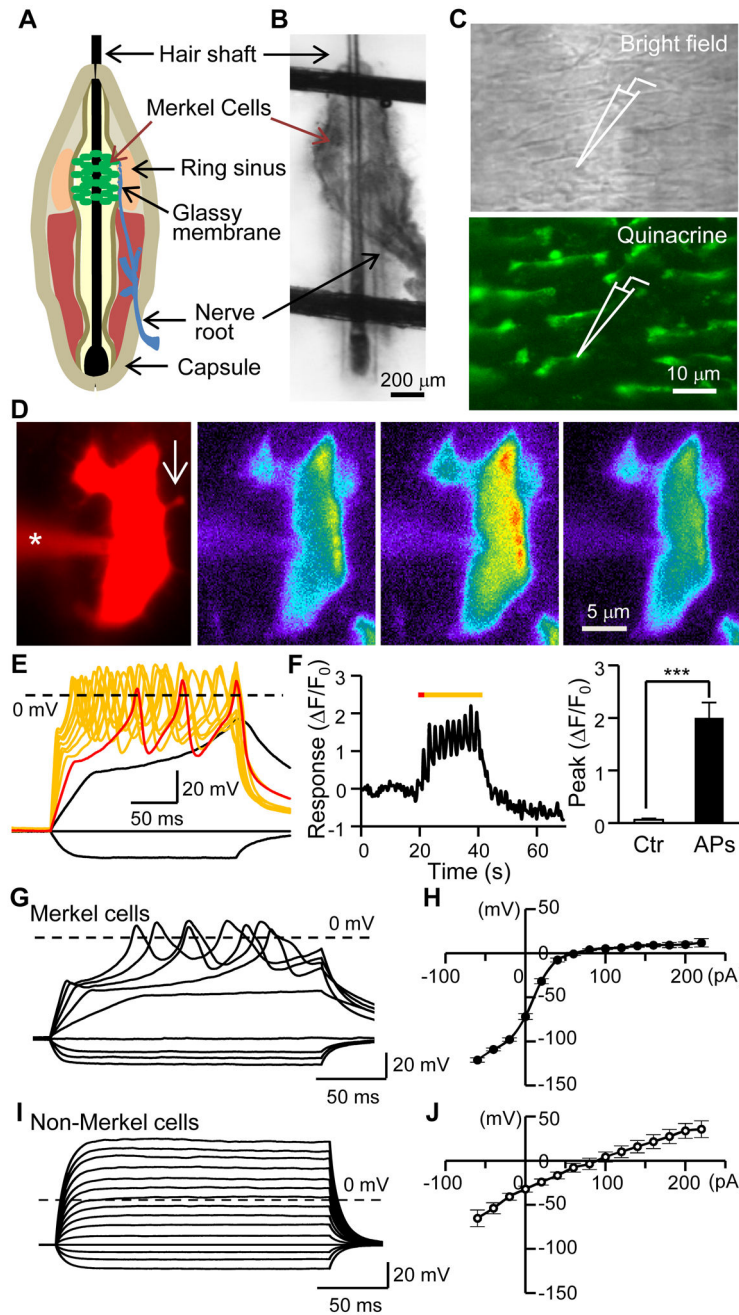


Figure 1. Merkel cells *in situ* fire action potentials

(A) Whisker hair follicle structure. (B) Image shows a fresh whisker hair follicle anchored in a recording chamber for patch-clamp recordings; the capsule of the hair follicle was removed. (C) Top, Merkel cell layer after peeling off the glassy membrane. Bottom, Quinacrine vital-staining for pre-identifying Merkel cells for patch-clamp recordings. (D) A quinacrine-stained cell *in situ* was filled with both Alexa 555 and Fluo-3 through a recording electrode (indicated by *). The arrow in the first image indicates a cell process viewed with Alexa 555. The Ca^{2+} imaging shows Fluo-3 fluorescence before (2nd image), during (3rd image), and after (4th image) action potential (AP) firing (illustrated in E). (E) Injection of depolarizing currents elicited AP firing (superimposed colored traces) in the Merkel cell. The red trace is the response to a 40-pA current step. (F)

Time course (left) of Fluo-3 intensity of the cell in **E** and summary data (right, $n = 7$, Ctr, control before APs). Colored line in left panel indicates the period of 10 supra-threshold depolarizing steps. (**G&H**) Sample traces of membrane responses and AP firing in response to depolarizing current steps in a Merkel cell (**G**) and summary data of V-I relationship of 48 Merkel cells (**H**, $n = 48$). (**I&J**) Sample traces of membrane responses to depolarizing current steps in a non-Merkel cell (**I**) and summary data of V-I relationship of 19 non-Merkel cells (**J**, $n = 19$). Data represent the mean \pm SEM. *** $P < 0.001$, paired Student t-test. See also Table S1.

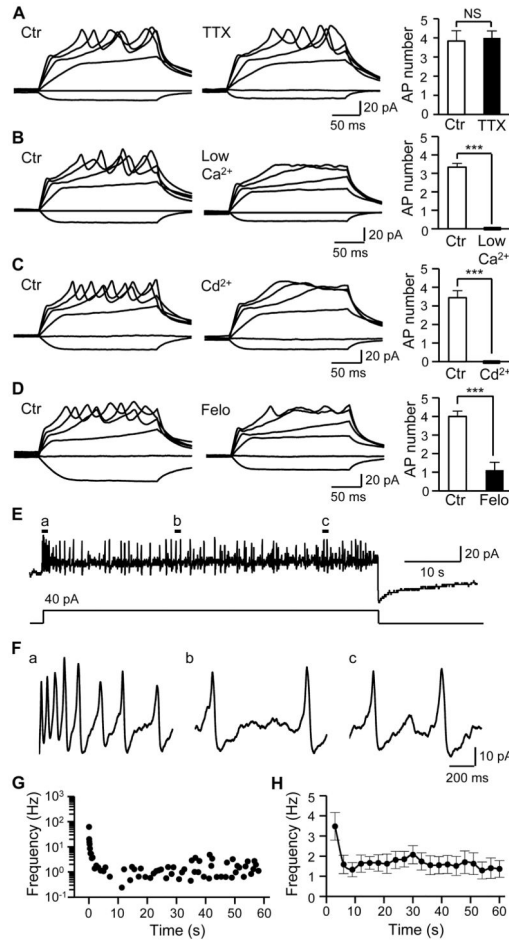


Figure 2. Merkel cells fire slowly adapting Ca²⁺-action potentials

(A) Merkel cell APs in the absence (left) and presence (middle) of 0.5 μM TTX. Right panel, summary data ($n = 6$). (B) Merkel cell APs depend on extracellular Ca²⁺. Left panel, APs in normal Krebs solution ($[\text{Ca}^{2+}]_o = 2.5 \text{ mM}$). Middle panel, failure to fire APs in a bath solution with low extracellular Ca²⁺ (20 μM). Right Panel, summary data ($n = 6$). (C) Merkel cell APs are abolished by Ca²⁺ channel blocker Cd²⁺. Left, in the absence of Cd²⁺; Middle panel, in the presence of 300 μM Cd²⁺, Right panel, summary data ($n = 9$). (D) Merkel cell APs are abolished by L-type VGCC blocker felodipine (Felo). Left panel, in the absence of felodipine; Middle panel, in the presence of 0.1 μM felodipine, Right panel, summary data ($n = 9$). (E) Merkel cell APs in response to a 1-min depolarizing current step at 40 pA. The recording was performed in normal Krebs solution. (F) APs at an expanded scale in the a, b, and c locations indicated in E. (G) Representative plots of instantaneous AP frequency over the 1-min recording shown in E. (H) Summary data for the experiments represented in E. The frequency at each point is calculated with a time bin of 3 sec. Results are pooled from 11 Merkel cells ($n = 11$). Data represent the mean \pm SEM. NS, no significant difference; *** $P < 0.001$, paired Student t-test. See also Figure S1.

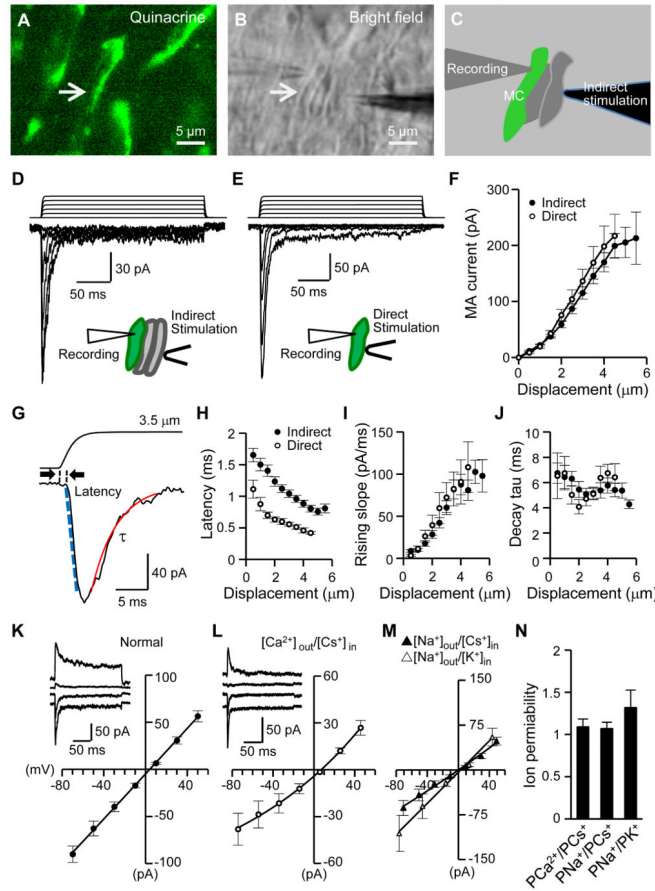


Figure 3. Touching follicle tissues evokes MA currents in Merkel cells

(A–C) The configuration of indirect displacement stimulation during patch-clamp recordings from Merkel cells *in situ*. The arrow indicates a quinacraine-stained Merkel cell in fluorescent image (A) and bright field (B). The Merkel cell and two adjacent cells are outlined in C. The mechanical impact is transmitted to the recorded Merkel cell via adjacent cells when the stimulation probe moves forward. (D&E) Whole-cell mechanically activated currents (MA) recorded from two Merkel cells stimulated by either indirect displacement (D) or direct displacement (E). Displacement step, 1 μm . $V_h = -75$ mV. (F) Summary data of MA amplitude at different distances of indirect displacement ($n = 28$) or direct displacement ($n = 9$). Displacement step, 0.5 μm . (G)

Sample traces of dual recording of piezo probe movement (top) and MA current (bottom) at an expanded time scale. (H–J) Summary data of latency, rising slope, and decay time constant (τ) at different displacement distances. Closed circle, indirect displacement ($n = 28$); open circle, direct displacement ($n = 9$). (K–N) I–V relationships of MA currents under normal recording condition (K, $E_{\text{rev}} = 1.1 \pm 1.2$ mV, $n = 21$), under $[\text{Ca}^{2+}]_{\text{out}}/[\text{Cs}^+]_{\text{in}}$ (L, $E_{\text{rev}} = 7.0 \pm 1.3$ mV, $n = 7$), $[\text{Na}^+]_{\text{out}}/[\text{Cs}^+]_{\text{in}}$ (M, $E_{\text{rev}} = 1.3 \pm 1.9$ mV, $n = 7$) and $[\text{Na}^+]_{\text{out}}/[\text{K}^+]_{\text{in}}$ (N, $E_{\text{rev}} = 5.1 \pm 4$ mV, $n = 7$) recording conditions. Insets in K and L are sample traces of MA currents. (N) Ion permeability: $\text{PCa}^{2+}/\text{PCs}^+ = 1.1 \pm 0.1$ ($n = 7$), $\text{PNa}^+/\text{PCs}^+ = 1.1 \pm 0.1$ ($n = 7$), and $\text{PNa}^+/\text{PK}^+ = 1.3 \pm 0.2$ ($n = 7$). Data represent the mean \pm SEM. See also Figure S2.

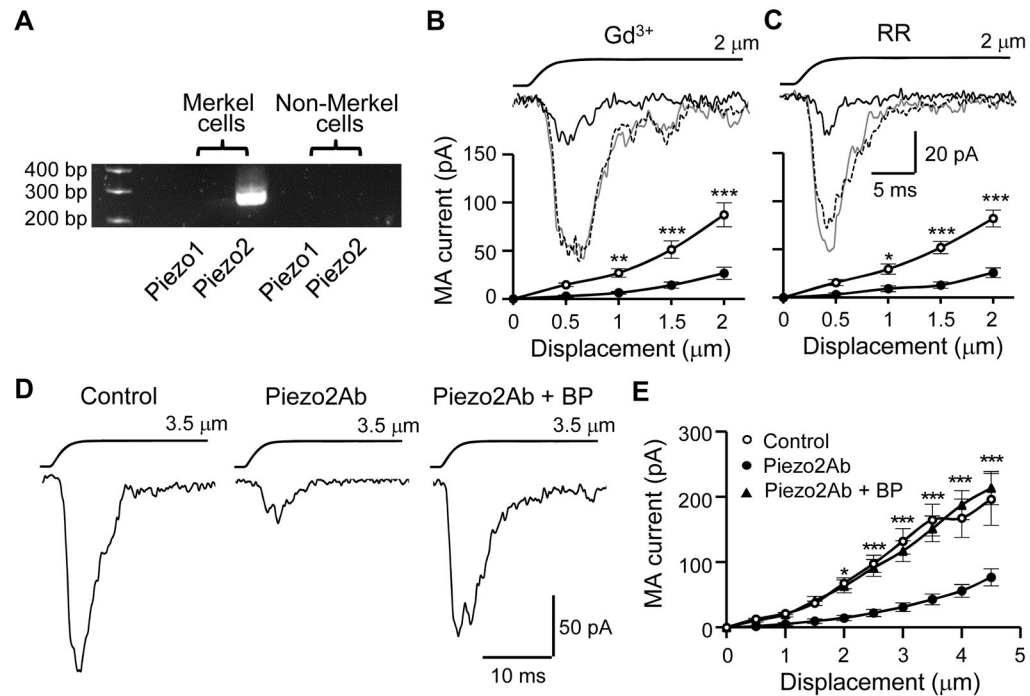


Figure 4. Expression of Piezo2 ion channels in Merkel cells and pharmacological properties of MA currents in Merkel cells (A) RT-PCR shows Piezo2 mRNA in Merkel cells. (B&C) Inhibition of MA currents in Merkel cells by 30 μM Gd^{3+} (B, n = 11) and 30 μM RR (C, n = 9). Sample traces (inset) represent MA currents before (gray line), 10 min following the bath application of Gd^{3+} or RR (black line), and after wash off (dashed line). The graphs are MA currents before (○) and following (●) the bath applications of the blockers. Indirect displacements were applied. (D) Sample traces of MA currents in the absence (control), presence of a Piezo2 antibody (Piezo2Ab), and the presence of the Piezo2Ab plus its blocking peptide (BP). MA currents were recorded 10 min after establishing the whole-cell mode and indirect displacement was applied at 3.5 μm . (E) Comparison of MA current amplitudes recorded 10 min after establishing the whole-cell mode. Control, n = 9; Piezo2Ab, n = 17; piezo2Ab+BP, n = 12. In D and E Piezo2Ab or Piezo2Ab+BP was applied through the patch-clamp internal recording solution. Data represent the mean \pm SEM. * $P < 0.05$, ** $P < 0.01$, *** $P < 0.001$, two-way ANOVA with Bonferroni post-hoc tests. See also Figure S3.

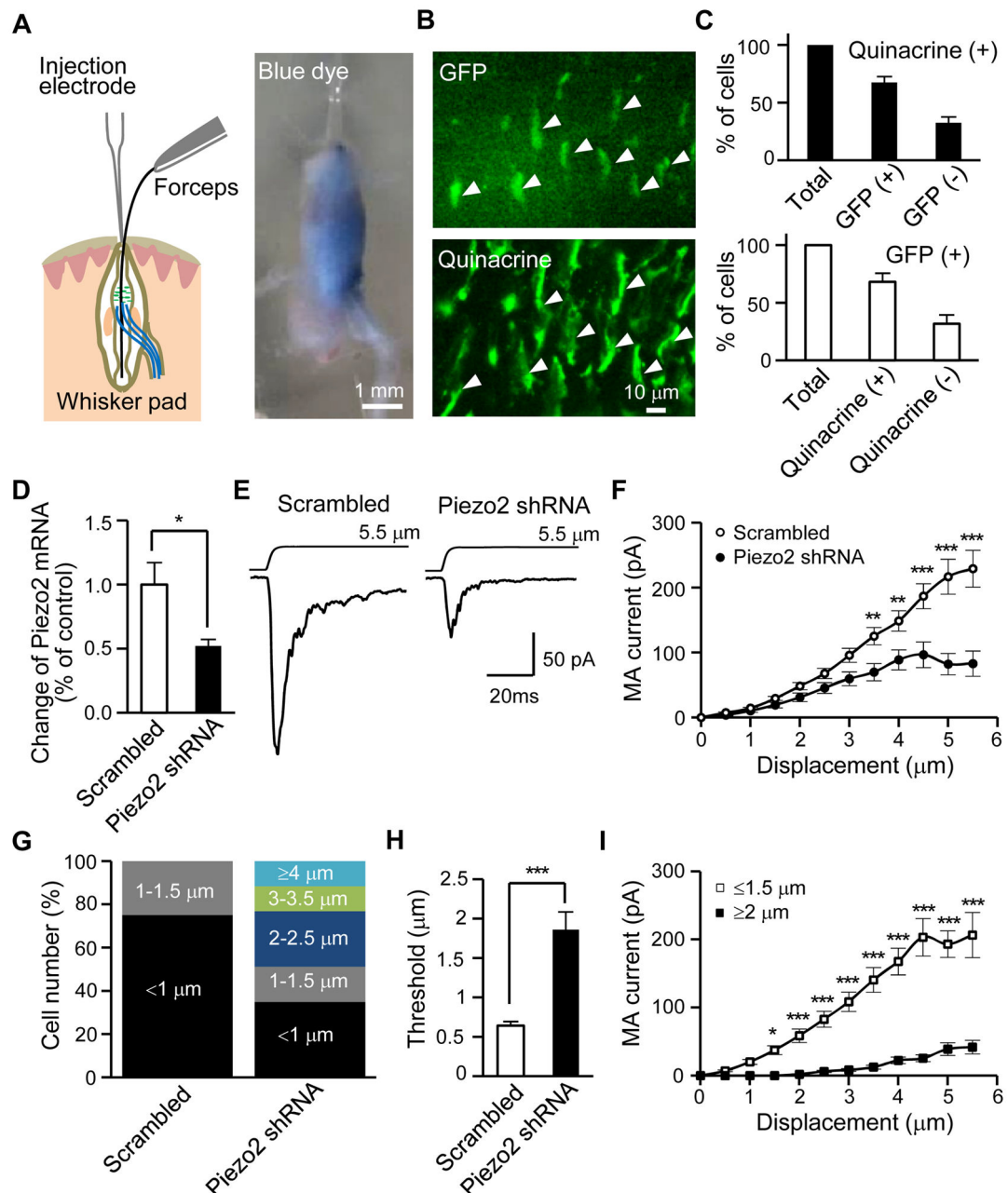


Figure 5. MA currents in Merkel cells are specifically reduced by knockdown of Piezo2 ion channels

(A) Left, schematic illustration of intra-follicle injection. Right, a whisker hair follicle after the injection of a blue dye solution ($\sim 3 \mu\text{l}$), it shows that the solution is injected into the whisker hair follicle and remains inside. (B) Top, lentiviral particle-mediated GFP expression in a whisker hair follicle 10 days after intra-follicle injection of GFP lentiviral particles. Bottom, the same field following quinacrine staining. Note that quinacrine fluorescent intensity is stronger than GFP so that GFP and quinacrine staining could be imaged sequentially. (C) Top, percentage of GFP-positive and -negative cells among 218 quinacrine-stained cells (8 follicles). Bottom, percentage of quinacrine-stained or non-stained cells among 202 GFP-positive cells (8 follicles). (D) Quantitative PCR measurement of the changes of Piezo2 mRNA in the enlargement segments of whisker hair follicles. Open bar: control group following intra-follicle injection of scrambled shRNA lentiviral particles ($n = 4$, triplicate

for each sample). Solid bar: whisker hair follicles that received intra-follicle injection of Piezo2 shRNA lentiviral particles (n = 4, triplicate for each sample). **(E)** Traces represent averaged MA currents in Merkel cells following intra-follicle application of lentiviral particles with either scrambled shRNA (left, n = 17) or Piezo2 shRNA (right, n = 20). **(F)** Summary data for scrambled or Piezo2 shRNA groups. **(G)** Percentage of Merkel cells with different thresholds following scrambled or Piezo2 shRNA. **(H)**

Summary of mechanotransduction thresholds for scrambled or Piezo2 shRNA groups. From **F** to **H**, cell numbers are 28 for scrambled shRNA group and 43 for Piezo2 shRNA group. **(I)** MA amplitudes of high threshold Merkel cells ($> 2.0 \mu\text{m}$, 21 cells) or low threshold Merkel cells ($< 1.5 \mu\text{m}$, 22 cells) in Piezo2 shRNAs group. Data represent the mean \pm SEM. * $P < 0.05$, ** $P < 0.01$, *** $P < 0.001$, Student's t-test or two-way ANOVA with Bonferroni post-hoc tests. See also Figure S4 and Figure S5.

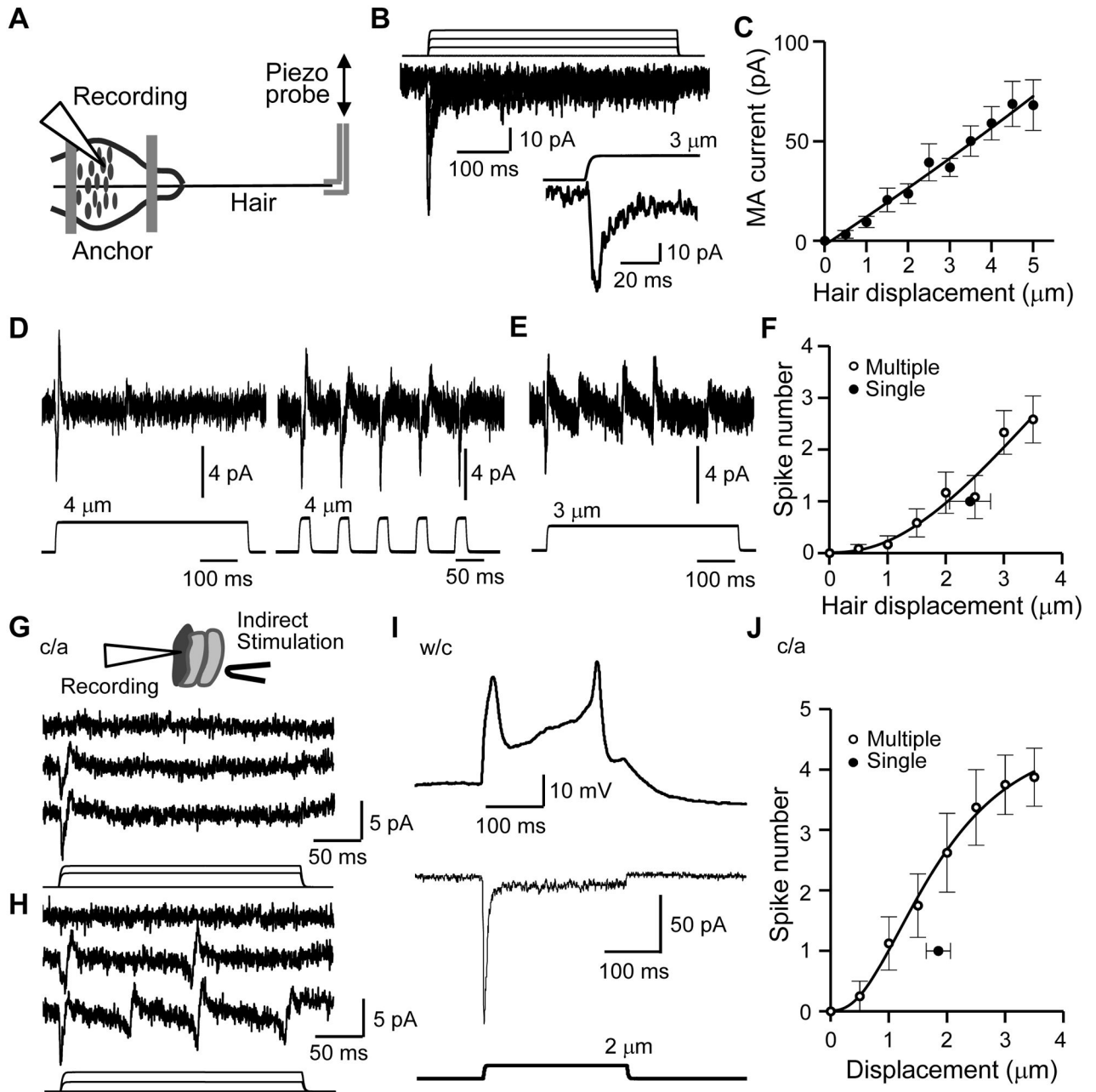


Figure 6. Gently touching whisker hairs or follicle tissues induces action potential firing in Merkel cells

(A–F) Gently touching whisker hairs induces MA currents and AP firing in Merkel cells *in situ*. (A) Recording setup. (B) MA currents in a Merkel cell elicited by hair displacement (1.0 μm increments). Inset, at an expanded time scale. (C) Summary data ($n = 15$). (D) Left, a single AP spike in a Merkel cell evoked by a single 500-ms hair movement. Right, 5 spikes elicited by 5 25-ms stimuli. Recordings were under cell-attached mode with hair displacement of 4 μm . (E) Multiple AP spikes in a Merkel cell induced by a 500-ms hair displacement at 3 μm . (F) Summary data. The single closed circle shows threshold ($2.4 \pm 0.4 \mu\text{m}$, $n = 5$) for the single AP spike cells. The open circles show the relationship between hair displacement distance and AP spike number for the cells with multiple AP spikes. The mean threshold is $2.2 \pm 0.3 \mu\text{m}$ ($n = 5$).

(G–J) Indirectly displacing Merkel cells induces AP firing in Merkel cells *in situ*. (G) AP spike currents recorded from a Merkel cell in response to indirect stimulation.

The AP spikes are recorded under the cell-attached (c/a) mode. Traces from the top to the bottom are baseline, and responses following displacement steps of 2 and 3 μm . The bottom panel shows the displacement steps. **(H)** Similar to **G** except that this cell has graded responses with multiple AP spikes. Displacement steps are 1 and 2 μm . **(I)** Same cell as **H** after breaking into the whole-cell (w/c) mode, a 2- μm displacement step elicits APs (top trace) in the current-clamp mode and an inward current (bottom trace) in voltage-clamp mode ($V_h = -75 \text{ mV}$). Similar results were obtained in 9 other Merkel cells. **(J)** Summary of AP spikes recorded under the cell-attached mode. The single closed circle shows the threshold ($1.9 \pm 0.2 \mu\text{m}$, $n = 20$) for the Merkel cells that only fired a single spike. Single AP spike cells are arbitrarily defined as the Merkel cells that fired only a single spike following an additional 3 forward displacement steps (0.5 μm increment each) above the threshold. The open circles show the relationship between displacement distances and spike numbers in the cells that had graded responses ($n = 8$); the threshold is $1.4 \pm 0.2 \mu\text{m}$ ($n = 8$). Displacement steps were applied for 250 ms in each test. Data represent the mean \pm SEM.

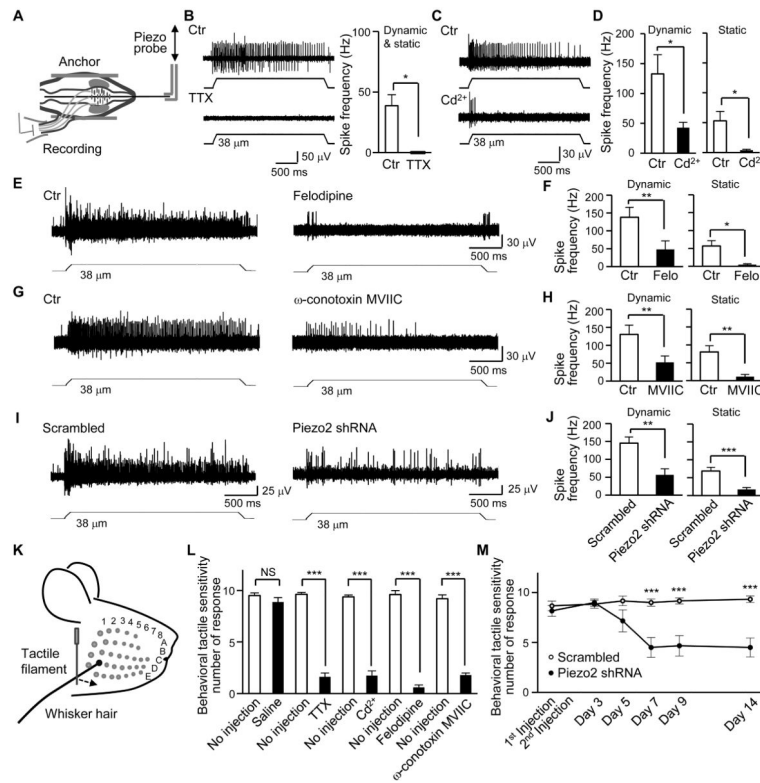


Figure 7. Inhibition of Merkel cell Ca^{2+} -action potentials suppresses SAI responses, and Ca^{2+} -action potentials and Piezo2 are required for behavioral tactile sensitivity

(A) Setup for whisker afferent recordings. (B) Left panel, sample traces of SAI responses before (Ctr, top) and following bath application of $0.5 \mu\text{M}$ TTX (bottom). Right panel, Summary data ($n = 5$). (C) Sample traces of SAI responses before (Ctr, top) and following bath application of $300 \mu\text{M}$ Cd^{2+} (bottom). (D) Summary data ($n = 7$) of the experiments represented in C. Open and closed bars are SAI frequency before and following Cd^{2+} application, respectively. Left panel, dynamic phase; Right panel, static phase. (E) Sample traces of SAI responses before (Ctr, left) and following bath application of $0.1 \mu\text{M}$ felodipine (right).

(F) Summary data ($n = 6$) of the experiments represented in E. (G) Sample traces of SAI responses before (Ctr, left) and following bath application of $1 \mu\text{M}$ ω -conotoxin (right). (H) Summary data ($n = 6$) of the experiments represented in G. (I) Sample traces of SAI responses in scrambled shRNA group (left) and Piezo2 shRNA group (right). (J) Summary data of the experiments represented in I, $n = 12$ for scrambled shRNA group, $n = 12$ for Piezo2 shRNA group. Hair displacement was $38\text{-}\mu\text{m}$ From B–J. (K) Schematic illustration of the whisker tactile test. (L) Behavioral tactile responses to whisker tactile stimulation under the following conditions: no injection ($n = 8$), intra-follicle injections of saline ($3 \mu\text{l}$, $n = 8$), TTX ($0.048 \mu\text{g}$, $n = 8$), Cd^{2+} ($33 \mu\text{g}$, $n = 8$), felodipine ($0.058 \mu\text{g}$, $n = 6$), or ω -conotoxin MVIIC ($2.8 \mu\text{g}$, $n = 5$).

(M) Behavioral tactile responses to whisker tactile stimulation in rats following intra-follicle injection of Piezo2 shRNA lentiviral particles ($n = 6$) or scrambled shRNA lentiviral particles ($n = 6$). In Both L and M, prior to each behavioral experiment, capsaicin was injected subcutaneously into facial areas of the testing rats to facilitate quantitatively measuring tactile responses. Data represent the mean \pm SEM. $*P < 0.05$, $**P < 0.01$, $***P < 0.001$, paired or unpaired Student's t-test or two-way ANOVA with Bonferroni post-hoc tests. See also Figure S6 and Figure S7.